PROCEEDINGS A

royalsocietypublishing.org/journal/rspa

Research

Cite this article: Chapman CJ, Sorokin SV. 2021 A Wronskian method for elastic waves propagating along a tube. *Proc. R. Soc. A* **477**: 20210202.
https://doi.org/10.1098/rspa.2021.0202

Received: 11 March 2021
Accepted: 13 May 2021

Subject Areas:
mathematical modelling, mechanics, wave motion

Keywords:
dispersion relation, dominant balance, group velocity, shell theory, ring frequency

Author for correspondence:
C. J. Chapman
e-mail: c.j.chapman@keele.ac.uk

Downloaded from https://royalsocietypublishing.org/ on 09 June 2021

A Wronskian method for elastic waves propagating along a tube

C. J. Chapman[1] and S. V. Sorokin[2]

[1]Department of Mathematics, University of Keele, Staffordshire ST5 5BG, UK
[2]Faculty of Engineering and Science, Aalborg University, Fibigerstraede 16, 9220 Aalborg, Denmark

CJC, 0000-0002-1530-1426

A technique involving the higher Wronskians of a differential equation is presented for analysing the dispersion relation in a class of wave propagation problems. The technique shows that the complicated transcendental-function expressions which occur in series expansions of the dispersion function can, remarkably, be simplified to low-order polynomials exactly, with explicit coefficients which we determine. Hence simple but high-order expansions exist which apply beyond the frequency and wavenumber range of widely used approximations based on kinematic hypotheses. The new expansions are hypothesis-free, in that they are derived rigorously from the governing equations, without approximation. Full details are presented for axisymmetric elastic waves propagating along a tube, for which stretching and bending waves are coupled. New approximate dispersion relations are obtained, and their high accuracy confirmed by comparison with the results of numerical computations. The weak coupling limit is given particular attention, and shown to have a wide range of validity, extending well into the range of strong coupling.

1. Introduction

The most common approach to analysing long wave propagation in a waveguide is to make at the outset a kinematic assumption about the shape of the field. This gives excellent results if the frequency and wavenumber are low enough, for example in an elastic waveguide when the motion is such that 'plane sections remain plane' [1–4]. Yet inevitably, as the kinematic assumption

THE ROYAL SOCIETY PUBLISHING

© 2021 The Author(s) Published by the Royal Society. All rights reserved.

Downloaded from https://royalsocietypublishing.org/ on 09 June 2021

starts to break down at higher frequencies and wavenumbers, the method must lose accuracy and ultimately fail, and it provides no way of finding a sequence of corrections.

An alternative is to start with the equations of motion and analyse their solutions where these are available. For example, in linear problems with circular cylindrical geometry, the solutions are often expressible in terms of Bessel functions, and the dispersion relation is then of determinant form with entries evaluated at the waveguide boundaries [5,6]. In principle, the determinant may be expanded in powers of the thickness of the waveguide, regarded as a small parameter, to give a sequence of approximations to the dispersion relation. The terms in this sequence make it possible first to check the validity of results obtained from a kinematic assumption, and second to extend these results to higher frequency and wavenumber by including more terms in the series.

In practice, two difficulties arise in carrying out the above procedure. The first is that many low order terms cancel, so that to obtain even a leading-order approximation can be beyond the reach of hand calculation. However, this difficulty for our predecessors is now by-passed by the use of algebraic software such as Mathematica, in which a short code can produce all the required terms up to high order in at most a few minutes. The second difficulty is that the exact coefficients in the thickness expansion are extremely complicated expressions in Bessel functions and their derivatives. Thus at first sight the expansion is too unwieldy to be of use. The key finding of the present paper is that by means of a mathematical technique involving identities in the higher Wronskians of the underlying differential equations, all of these expressions may be shown to simplify unexpectedly to low-order polynomials, moreover with simple coefficients which are easily calculated exactly. These identities do not appear in reference works (e.g. [7–9]) and appear to be new.

A crucial aspect of the resulting series expansion is that the coefficients involve no assumption that the frequency or wavenumber is small; the expansion is merely in the thickness, and the coefficients are explicit low-order polynomials in the frequency and wavenumber, without any approximation. This remarkable analytic structure, far simpler than might have been anticipated from the transcendental starting point, is the key to the new results presented here. It enables us readily to determine the range of frequency and wavenumber for which a given truncation of the series is accurate, by choosing appropriate scaling and considering the relative magnitude of successive terms in the series [10,11]. The accurate numerical determination of this range, for the most useful truncations, is an important part of the present paper, and is of particular relevance to applications.

The paper is arranged as follows. Section 2 gives the required theory for the curved waveguide to be considered, namely an elastic cylindrical tube, using Bessel functions to describe axisymmetric elastic waves propagating along the tube. Before deformation, the tube wall occupies a cylindrical annulus. Section 3 analyses the resulting dispersion relation, with attention to its analytic structure when expanded in powers of the wall thickness. We derive from first principles the Wronskian identities required. Section 4 shows how the thickness expansion gives not only the classical approximation to the dispersion relation for a thin cylindrical shell but also a family of correction terms to it. A noteworthy feature of the exact dispersion relation is a prominent avoided crossing [12,13]: two main branches approach each other, but then veer away. Sections 5–8 analyse the avoided crossing mathematically by first considering a special limit of no coupling between two types of wave supported by the waveguide. In this limiting case, the dispersion relation factorizes, and crossing occurs. A perturbation analysis then gives a weak coupling theory, providing several new families of approximations, suitable for different regions of the frequency–wavenumber plane. These are shown numerically to have a wide range of validity, in that they remain accurate even when the coupling is quite strong. Section 9 presents conclusions, especially regarding the scope of the Wronskian method in further work on waveguide theory. The method is not restricted to elastic waves, but applies equally to waves in fluid dynamics or electromagnetism, for example, provided there exists an underlying equation for which a Wronskian can be defined.

royalsocietypublishing.org/journal/rspa Proc. R. Soc. A 477: 20210202

Downloaded from https://royalsocietypublishing.org/ on 09 June 2021

2. Elastic waves in a cylindrical tube

(a) Governing equations

We shall follow the notation of [6] and write the equation for the displacement $\mathbf{u}$ of a wave in an isotropic elastic medium in the form

$$\frac{\partial^2 \mathbf{u}}{\partial t^2} = (c_1^2 - c_2^2)\nabla\nabla\cdot\mathbf{u} + c_2^2\nabla^2\mathbf{u}. \tag{2.1}$$

The compression wave speed is c_1 and the shear wave speed is c_2, defined in terms of a reference speed c_0 by

$$c_1 = \left\{\frac{1-\nu}{(1+\nu)(1-2\nu)}\right\}^{1/2} c_0, \quad c_2 = \frac{c_0}{\{2(1+\nu)\}^{1/2}}, \quad c_0 = \left(\frac{E}{\rho}\right)^{1/2}, \tag{2.2}$$

where is ν is Poisson's ratio, E is Young's modulus, and ρ is the density. The tube wall is taken to have thickness h, mean radius a, inner radius $a_\mathrm{i} = a - h/2$ and exterior radius $a_\mathrm{e} = a + h/2$. The dimensionless thickness is $\epsilon = h/a$, and for a wave of frequency ω, the dimensionless frequency is $\Omega = \omega a/c_0$. In cylindrical coordinates (r, θ, z), the displacement is $\mathbf{u} = (u, v, w)$, and t denotes time. The tube wall occupies the region $a_\mathrm{i} < r < a_\mathrm{e}$.

Our analysis is for axisymmetric waves without circumferential displacement, i.e. with $v = 0$. Such waves may be written in terms of potentials $\hat\phi = \hat\phi(r, z, t)$ and $\hat\chi = \hat\chi(r, z, t)$ as [14, p. 1766]

$$\mathbf{u} = \nabla\hat\phi + \nabla\times\nabla\times(\hat\chi\,\mathbf{e}_z), \tag{2.3}$$

where $\mathbf{e}_z$ is a unit vector in the z direction. These potentials separate compression from shear in the bulk wave equations

$$\frac{\partial^2\hat\phi}{\partial t^2} = c_1^2\nabla^2\hat\phi, \quad \frac{\partial^2\hat\chi}{\partial t^2} = c_2^2\nabla^2\hat\chi, \tag{2.4}$$

so that coupling occurs only at the boundaries $r = a_\mathrm{i}$ and $r = a_\mathrm{e}$. In terms of the strain components

$$e_{rr} = \frac{\partial u}{\partial r}, \quad e_{\theta\theta} = \frac{u}{r}, \quad e_{zz} = \frac{\partial w}{\partial z}, \quad e_{rz} = \frac{1}{2}\left(\frac{\partial w}{\partial r} + \frac{\partial u}{\partial z}\right), \tag{2.5}$$

traction-free boundary conditions are $\tau_{rr} = 0$ and $\tau_{rz} = 0$, where

$$\tau_{rr} = \rho\{c_1^2 e_{rr} + (c_1^2 - 2c_2^2)(e_{\theta\theta} + e_{zz})\}, \quad \tau_{rz} = 2\rho c_2^2 e_{rz}. \tag{2.6}$$

(b) Wave propagation

We consider displacements proportional to $\mathrm{e}^{-\mathrm{i}\omega t + \mathrm{i}kz}$, and omit this factor throughout. The remaining part is a function of r only, so that

$$\hat\phi = \mathrm{i}\phi(r), \quad \hat\chi = \chi(r) \tag{2.7}$$

and

$$\nabla\hat\phi = (\mathrm{i}\phi_r, -k\phi), \quad \nabla\times\nabla\times(\hat\chi\,\mathbf{e}_z) = \left(\mathrm{i}k\chi_r, -\frac{1}{r}(r\chi_r)_r\right). \tag{2.8}$$

Here, the subscript r denotes differentiation with respect to r. The frequency ω is real, but the wavenumber k may be complex. By (2.3), the displacement is

$$(u, w) = \left(\mathrm{i}\phi_r + \mathrm{i}k\chi_r, -k\phi - \frac{1}{r}(r\chi_r)_r\right), \tag{2.9}$$

from which (2.5) and (2.6) give the strain and stress. Recall that the circumferential displacement is zero. The bulk equations (2.4) are

$$r^2\phi_{rr} + r\phi_r + \left\{\left(\frac{\omega r}{c_1}\right)^2 - (kr)^2\right\}\phi = 0 \tag{2.10}$$

Downloaded from https://royalsocietypublishing.org/ on 09 June 2021

and

$$r^2\chi_{rr} + r\chi_r + \left\{\left(\frac{\omega r}{c_2}\right)^2 - (kr)^2\right\}\chi = 0, \tag{2.11}$$

which are each a form of Bessel's equation of order zero, and the boundary conditions are

$$r\phi_r + \left\{\tfrac{1}{2}\left(\frac{\omega r}{c_2}\right)^2 - (kr)^2\right\}\phi = kr^2\chi_{rr} \tag{2.12}$$

and

$$\left\{\tfrac{1}{2}\left(\frac{\omega r}{c_2}\right)^2 - (kr)^2\right\}\chi_r = kr^2\phi_r. \tag{2.13}$$

The general solution of (2.10)–(2.11) involves Bessel functions J_0 and Y_0 evaluated at $\tilde{\Omega}_1 = \tilde{\Omega}_1(r) = \{(\omega r/c_1)^2 - (kr)^2\}^{1/2}$ or $\tilde{\Omega}_2 = \tilde{\Omega}_2(r) = \{(\omega r/c_2)^2 - (kr)^2\}^{1/2}$. We indicate which one by a subscript 1 or 2, so that $J_{0,2}$ represents $J_0(\tilde{\Omega}_2)$, for example. Any branch of the square roots may be used, since in the dispersion relation the square roots occur in pairs to leave an expression without branch points. Thus the solution of (2.10)–(2.11) is

$$\phi = A_1^{\mathrm{J}} J_{0,1} + A_1^{\mathrm{Y}} Y_{0,1} \tag{2.14}$$

and

$$\chi = \hat{A}_2^{\mathrm{J}} J_{0,2} + \hat{A}_2^{\mathrm{Y}} Y_{0,2}, \tag{2.15}$$

where A_1^{J}, A_1^{Y}, $\hat{A}_2^{\mathrm{J}}$ and $\hat{A}_2^{\mathrm{Y}}$ are modal coefficients. To obtain simpler formulae in what follows, we use the quantities $A_2^{\mathrm{J}} = k\hat{A}_2^{\mathrm{J}}$ and $A_2^{\mathrm{Y}} = k\hat{A}_2^{\mathrm{Y}}$, which have the same physical dimensions as A_1^{J} and A_1^{Y}; our starting-point (2.3) implies that the physical dimensions of ϕ and χ differ by a factor of a length.

The boundary conditions (2.12)–(2.13) applied at $r = a_{\mathrm{i}} = a - h/2$ and $r = a_{\mathrm{e}} = a + h/2$ may be written

$$A_1^{\mathrm{J}} d_{1\mathrm{i}}^{\mathrm{J}} + A_1^{\mathrm{Y}} d_{1\mathrm{i}}^{\mathrm{Y}} = -A_2^{\mathrm{J}} e_{2\mathrm{i}}^{\mathrm{J}} - A_2^{\mathrm{Y}} e_{2\mathrm{i}}^{\mathrm{Y}}, \tag{2.16}$$

$$A_1^{\mathrm{J}} d_{1\mathrm{e}}^{\mathrm{J}} + A_1^{\mathrm{Y}} d_{1\mathrm{e}}^{\mathrm{Y}} = -A_2^{\mathrm{J}} e_{2\mathrm{e}}^{\mathrm{J}} - A_2^{\mathrm{Y}} e_{2\mathrm{e}}^{\mathrm{Y}}, \tag{2.17}$$

$$A_1^{\mathrm{J}} f_{1\mathrm{i}}^{\mathrm{J}} + A_1^{\mathrm{Y}} f_{1\mathrm{i}}^{\mathrm{Y}} = -A_2^{\mathrm{J}} g_{2\mathrm{i}}^{\mathrm{J}} - A_2^{\mathrm{Y}} g_{2\mathrm{i}}^{\mathrm{Y}} \tag{2.18}$$

and

$$A_1^{\mathrm{J}} f_{1\mathrm{e}}^{\mathrm{J}} + A_1^{\mathrm{Y}} f_{1\mathrm{e}}^{\mathrm{Y}} = -A_2^{\mathrm{J}} g_{2\mathrm{e}}^{\mathrm{J}} - A_2^{\mathrm{Y}} g_{2\mathrm{e}}^{\mathrm{Y}}. \tag{2.19}$$

Here, we make use of the functions

$$d^{\mathrm{J}}(\tilde{\Omega}, K) = \tfrac{1}{2}(\tilde{\Omega}_2^2 - K^2)J_0(\tilde{\Omega}) + \tilde{\Omega}J_0'(\tilde{\Omega}), \tag{2.20}$$

$$e^{\mathrm{J}}(\tilde{\Omega}, K) = \tilde{\Omega}\{\tilde{\Omega}J_0(\tilde{\Omega}) + J_0'(\tilde{\Omega})\}, \tag{2.21}$$

$$f^{\mathrm{J}}(\tilde{\Omega}, K) = -K^2\tilde{\Omega}J_0'(\tilde{\Omega}) \tag{2.22}$$

and

$$g^{\mathrm{J}}(\tilde{\Omega}, K) = \tfrac{1}{2}(\tilde{\Omega}^2 - K^2)\tilde{\Omega}J_0'(\tilde{\Omega}), \tag{2.23}$$

and similarly $(d^{\mathrm{Y}}, e^{\mathrm{Y}}, f^{\mathrm{Y}}, g^{\mathrm{Y}})$, evaluated at the dimensionless frequencies

$$\tilde{\Omega}_{1\mathrm{i}} = \tilde{\Omega}_1(a_{\mathrm{i}}), \quad \tilde{\Omega}_{1\mathrm{e}} = \tilde{\Omega}_1(a_{\mathrm{e}}), \quad \tilde{\Omega}_{2\mathrm{i}} = \tilde{\Omega}_2(a_{\mathrm{i}}) \quad \text{and} \quad \tilde{\Omega}_{2\mathrm{e}} = \tilde{\Omega}_2(a_{\mathrm{e}}) \tag{2.24}$$

and wavenumbers $(K_{\mathrm{i}}, K_{\mathrm{e}}) = (ka_{\mathrm{i}}, ka_{\mathrm{e}})$ as indicated by subscripts; for example,

$$d_{1\mathrm{i}}^{\mathrm{J}} = d^{\mathrm{J}}(\tilde{\Omega}_{1\mathrm{i}}, K_{\mathrm{i}}) \quad \text{and} \quad g_{2\mathrm{e}}^{\mathrm{Y}} = g^{\mathrm{Y}}(\tilde{\Omega}_{2\mathrm{e}}, K_{\mathrm{e}}). \tag{2.25}$$

In the definition (2.20), the quantity $\tilde{\Omega}_2^2$ is not an argument of the function d^{J} (nor of d^{Y}); it is evaluated at $\tilde{\Omega}_{2\mathrm{i}}$ or $\tilde{\Omega}_{2\mathrm{e}}$, always with a subscript 2. This is a consequence of the way the term $(\omega r/c_2)^2$ enters the boundary conditions (2.12)–(2.13). In comparing the coefficients in (2.10)–(2.11) with those in (2.20)–(2.23), recall that the definitions of $\tilde{\Omega}_1^2$ and $\tilde{\Omega}_2^2$ include a term $-(kr)^2$.

Downloaded from https://royalsocietypublishing.org/ on 09 June 2021

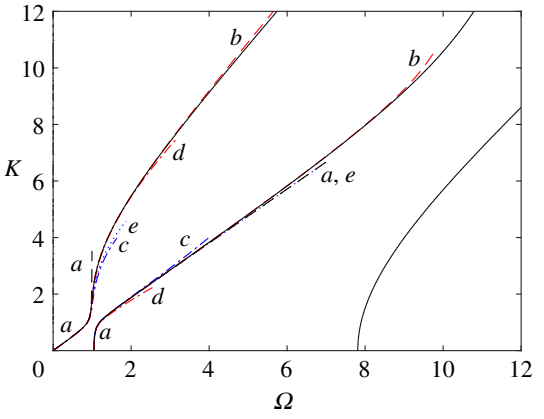

Figure 1. Dispersion relation for a cylindrical tube with Poisson's ratio $\nu = 0.3$ and dimensionless wall thickness $\epsilon = h/a = 0.25$. The axes are the radius-scaled frequency $\Omega = \omega a/c_0$ and wavenumber $K = ka$. Exact dispersion curves from the determinant equation (3.1) are solid, black; approximate curves and their equation numbers in the text are (*a*) (black, dashed): (3.19), (4.1); (*b*) (red, dashed): (4.4); (*c*) (blue, dash-dotted): (4.8); (*d*) (red, dash-dotted): (4.9); (*e*) (blue, dotted): (5.13). On the second branch, curves (*a*) and (*e*) are indistinguishable. The upper placings of the letters indicate the range of validity of the various approximations. For example, approximation (*a*) is valid up to about $K = 3$ on the first branch, and $K = 6$ on the second branch. Note the very wide range over which approximation (*b*) is accurate. (Online version in colour.)

3. The dispersion relation

The governing equations have a non-trivial solution when the determinant of equations (2.16)–(2.19) for the modal coefficients $(A_1^{\mathrm{J}}, A_1^{\mathrm{Y}}, A_2^{\mathrm{J}}, A_2^{\mathrm{Y}})$ is zero, i.e.

$$\begin{vmatrix} d_{1\mathrm{i}}^{\mathrm{J}} & d_{1\mathrm{i}}^{\mathrm{Y}} & e_{2\mathrm{i}}^{\mathrm{J}} & e_{2\mathrm{i}}^{\mathrm{Y}} \\ d_{1\mathrm{e}}^{\mathrm{J}} & d_{1\mathrm{e}}^{\mathrm{Y}} & e_{2\mathrm{e}}^{\mathrm{J}} & e_{2\mathrm{e}}^{\mathrm{Y}} \\ f_{1\mathrm{i}}^{\mathrm{J}} & f_{1\mathrm{i}}^{\mathrm{Y}} & g_{2\mathrm{i}}^{\mathrm{J}} & g_{2\mathrm{i}}^{\mathrm{Y}} \\ f_{1\mathrm{e}}^{\mathrm{J}} & f_{1\mathrm{e}}^{\mathrm{Y}} & g_{2\mathrm{e}}^{\mathrm{J}} & g_{2\mathrm{e}}^{\mathrm{Y}} \end{vmatrix} = 0. \tag{3.1}$$

As a relation between ω and k, this is the dispersion relation for axisymmetric waves with meridional displacement. Numerical evaluation of the determinant gives the first branches of the dispersion relation as the solid curves in figure 1, which is for Poisson's ratio $\nu = 0.3$ and dimensionless thickness $\epsilon = h/a = 0.25$. Our aim in what follows is to derive simple analytical approximations to this dispersion relation, valid in as wide a range of frequency and wavenumber as possible, by proceeding deductively from (3.1) rather than by making kinematic hypotheses.

When $K = 0$, the f terms defined by (2.22) are zero, and the block structure of (3.1) then gives a factorization into the product of the d terms and the g terms, i.e. as the product of two 2×2 determinants. These give the cut-on frequencies, separated into two families according to the type of displacement field. Later, we shall be interested in the special case $\nu = 0$, for which the two factors give the frequency equations

$$J''_{0,1\mathrm{i}}\, Y''_{0,1\mathrm{e}} - Y''_{0,1\mathrm{i}}\, J''_{0,1\mathrm{e}} = 0, \quad J'_{0,2\mathrm{i}}\, Y'_{0,2\mathrm{e}} - Y'_{0,2\mathrm{i}}\, J'_{0,2\mathrm{e}} = 0. \tag{3.2}$$

Here, $J''_{0,1\mathrm{i}} = J''_0(\Omega_{1\mathrm{i}})$, $Y''_{0,1\mathrm{e}} = Y''_0(\Omega_{1\mathrm{e}})$, etc., where $\Omega_{1\mathrm{i}} = \omega a_{\mathrm{i}}/c_1$ and $\Omega_{1\mathrm{e}} = \omega a_{\mathrm{e}}/c_1$, and similarly for the subscript 2, with c_2 instead of c_1. When $\nu = 0$, the definitions (2.2) give $c_1^2 = c_0^2$, $c_2^2 = c_0^2/2$, and $c_1^2 = 2c_2^2$; these relations are used in deriving (3.2).

Another feature of (3.1) when $\nu = 0$ is that it contains $\Omega^2 - K^2$ as a factor. This means that in the positive quadrant of the (frequency, wavenumber) plane, exact crossings are possible of the straight line $\Omega = K$ with other branches of the dispersion relation. A short analysis of (3.1), taking account of the many zero terms which occur, and using L'Hôpital's rule, shows that this occurs

Downloaded from https://royalsocietypublishing.org/ on 09 June 2021

when the frequency satisfies the first of equations (3.2). This is a remarkable result. It implies that for $\nu = 0$ the crossing frequencies are the same as those of one of the families of cut-on frequencies, even though in the dispersion plane these points are remote from each other, and have no obvious connection. We have checked numerically up to machine precision that in any dispersion diagram for $\nu = 0$, if a vertical line (parallel to the wavenumber axis) is drawn downwards from any crossing point, it does indeed intersect the frequency axis at a cut-on frequency; and moreover, the converse does not hold, in that the cut-on frequencies satisfying the second of equations (3.2) cannot be obtained in this way. We make use of these facts in §8 in checking series expansions for small Poisson's ratio.

(a) Expansion in powers of the thickness

We now derive a series expansion of the dispersion relation in powers of the dimensionless thickness $\epsilon = h/a$. The quantities defined in and after (2.24) may be expressed in terms of central values $(\tilde{\Omega}_{1a}, \tilde{\Omega}_{2a}, K) = (\tilde{\Omega}_1(a), \tilde{\Omega}_2(a), ka)$ as

$$(\tilde{\Omega}_{1i}, \tilde{\Omega}_{2i}, K_i) = (1 - \tfrac{1}{2}\epsilon)(\tilde{\Omega}_{1a}, \tilde{\Omega}_{2a}, K), \tag{3.3}$$

and similarly for $(\tilde{\Omega}_{1e}, \tilde{\Omega}_{2e}, K_e)$ with $1 + \frac{1}{2}\epsilon$ instead of $1 - \frac{1}{2}\epsilon$. The individual entries in the determinant (3.1) have series expansions in ϵ in which the coefficients involve the Bessel functions (J_0, Y_0) and their derivatives evaluated at $\tilde{\Omega}_{1a}$ and $\tilde{\Omega}_{2a}$. Hence the full determinant also has a series expansion of this type.

At first sight, the series so obtained would appear to be of limited use because it involves complicated expressions in high derivatives of Bessel functions. However, the symmetry of the basic determinant (3.1) is such that the Bessel functions occur only in certain combinations which we shall call higher Wronskians, and which are all expressible as polynomials in the reciprocal of their arguments. Hence the series simplifies to a quite remarkable extent, and is in fact of considerable use, not least in providing a rigorous check of the validity of any result derived from a kinematic hypothesis. It must be emphasized that the coefficients finally obtained in the series expansion in ϵ are exact polynomial expressions in the frequency and wavenumber; they are not truncations of infinite series. That this occurs is a new feature of the present work.

(b) Wronskian identities

The Wronskian $W = W(s)$ of Bessel functions $(J_\mu, Y_\mu) = (J_\mu(s), Y_\mu(s))$ is [9, p. 222]

$$W = J_\mu Y'_\mu - J'_\mu Y_\mu = \frac{2}{\pi s}, \tag{3.4}$$

where a prime denotes the derivative with respect to s. On differentiating this relation repeatedly with respect to s, a set of identities is obtained which can be expressed in terms of the higher Wronskians $W_{mn} = W_{mn}(s)$ defined for non-negative integers m and n by $W_{mn} = J^{(m)}_\mu Y^{(n)}_\mu - J^{(n)}_\mu Y^{(m)}_\mu$. The first two of these identities are

$$W_{02} = -\frac{2}{\pi s^2}, \qquad W_{03} + W_{12} = \frac{4}{\pi s^3}. \tag{3.5}$$

The original Wronskian is $W = W_{01}$, and we also have the basic relations

$$W_{mn} = -W_{nm}, \quad W'_{mn} = W_{m+1,n} + W_{m,n+1}. \tag{3.6}$$

In particular, $W_{mm} = 0$ and $W'_{m,m+1} = W_{m,m+2}$ for all m. We shall often omit the term 'higher' when referring to higher Wronskians.

Downloaded from https://royalsocietypublishing.org/ on 09 June 2021

A further set of identities is obtained by successively differentiating and cross-multiplying Bessel's equation for J_μ and Y_μ, i.e.

$$pJ''_\mu + qJ'_\mu + rJ_\mu = 0 \quad \text{and} \quad pY''_\mu + qY'_\mu + rY_\mu = 0. \tag{3.7}$$

Here $p = s^2$, $q = s$ and $r = s^2 - \mu^2$. (The variable r has temporarily a different meaning from earlier.) The first two derivatives of the equation for J_μ, for example, are

$$pJ^{(3)}_\mu + (p' + q)J''_\mu + (q' + r)J'_\mu + r'J_\mu = 0 \tag{3.8}$$

and

$$pJ^{(4)}_\mu + (2p' + q)J^{(3)}_\mu + (p'' + 2q' + r)J''_\mu + 2r'J'_\mu + r''J_\mu = 0, \tag{3.9}$$

and likewise for the Y_μ equations, with the same coefficients. Continuing in this way, we obtain, for $m \geq 2$, a set of equations with first terms $pJ^{(m)}_\mu$ or $pY^{(m)}_\mu$. These equations contain binomial coefficients, because the terms arise from successive derivatives of products.

Let us say that if we multiply the $pY^{(n)}_\mu$ equation by $J^{(m)}_\mu$, and subtract the $pJ^{(n)}_\mu$ equation multiplied by $Y^{(m)}_\mu$, where $n \geq 2$ and $m \geq 0$, the result is the (m, n) equation. Then we obtain a set of linear equations in the higher Wronskians, in which the (m, n) equation begins with the term pW_{mn} (unless $m = n$, in which case the term is absent). The coefficients in these equations are the same as those in (3.8)–(3.9) and their higher derivatives. The set of Wronskians $W_{m'n'}$ appearing in these equations may be restricted to $n' > m'$, by the anti-symmetry property in (3.6); this has the effect of changing the sign of some of the terms.

For illustration, the first two identities for $m = 0$ are

$$pW_{02} + qW_{01} = 0 \tag{3.10}$$

and

$$pW_{03} + (p' + q)W_{02} + (q' + r)W_{01} = 0, \tag{3.11}$$

the first two for $m = 1$ are

$$pW_{12} - rW_{01} = 0 \tag{3.12}$$

and

$$pW_{13} + (p' + q)W_{02} - r'W_{01} = 0, \tag{3.13}$$

and the first two for $m = 2$ are

$$qW_{12} + rW_{02} = 0 \tag{3.14}$$

and

$$pW_{23} - (q' + r)W_{12} - r'W_{02} = 0. \tag{3.15}$$

From the definitions of p, q, r after (3.7), the only derivatives needed in the identities are $p' = r' = 2s$, $p'' = r'' = 2$ and $q' = 1$, since the higher derivatives are zero. In consequence, it is a simple matter to express all higher Wronskians in terms of the basic Wronskian $W = W_{01} = 2/(\pi s)$, and so obtain explicit formulae for the W_{mn} in terms of s and μ. It is evident from the structure of the equations that except for a factor of $1/\pi$ throughout, the W_{mn} are polynomials in $1/s$ with coefficients which are polynomials in μ. The calculation lends itself to a short Mathematica code. For example, some of the Wronskians for small (m, n) are

$$W_{03} = \frac{-2s^2 + 4 + 2\mu^2}{\pi s^3}, \quad W_{12} = \frac{2(s^2 - \mu^2)}{\pi s^3} \quad \text{and} \quad W_{13} = -\frac{2(s^2 - 3\mu^2)}{\pi s^4}, \tag{3.16}$$

and a Wronskian for somewhat higher (m, n) is

$$W_{34} = \frac{2s^6 - 6(1 + \mu^2)s^4 + 6\mu^2(2 + \mu^2)s^2 - 2\mu^2(4 - 5\mu^2 + \mu^4)}{\pi s^7}. \tag{3.17}$$

Not all of the identities are needed in calculating the W_{mn}. Those not needed are useful for checking the code, since evaluation of their left-hand sides, using previously computed quantities, must give zero.

Downloaded from https://royalsocietypublishing.org/ on 09 June 2021

(c) Series expansion of the dispersion relation

We saw after (3.3) that the dispersion relation has a series expansion in $\epsilon = h/a$ with coefficients involving the Bessel functions (J_0, Y_0) and their derivatives evaluated at the central values $\tilde{\Omega}_{1a}$ and $\tilde{\Omega}_{2a}$. This series in ϵ may be calculated in Mathematica, and then simplified by applying the above identities for $\mu = 0$. The result, which is far from obvious in advance, is that no individual Bessel functions or their derivatives remain: the coefficients in the series are polynomial expressions in the Wronskians $W_{mn}(\tilde{\Omega}_{1a})$ and $W_{mn}(\tilde{\Omega}_{2a})$, in combination with even powers of K, $\tilde{\Omega}_{1a}$ and $\tilde{\Omega}_{2a}$. On clearing of common factors, including a factor ϵ^2, the series takes the form

$$a_0 + a_2\epsilon^2 + a_4\epsilon^4 + \cdots = 0, \tag{3.18}$$

in which only even powers of ϵ occur, and the coefficient a_{2l} of ϵ^{2l} involves Wronskians W_{mn} up to $m + n = 2l + 3$. Thus to obtain the expansion up to order ϵ^4, for example, we need the Wronskians up to $m + n = 7$. The expressions for these Wronskians are short; for example, (3.17) shows that $W_{34}(s) = 2(s^2 - 3)/(\pi s^3)$ for $\mu = 0$. Thus the total simplification obtainable by the Wronskian method is very great.

It is convenient to express the coefficients a_{2l} in (3.18) in terms of the dimensionless frequency $\Omega = \omega a/c_0$ and use the notation $\alpha = (c_1/c_0)^2$ and $\beta = (c_2/c_0)^2$, so that $\tilde{\Omega}_{1a}^2 = \alpha^{-1}\Omega^2 - K^2$ and $\tilde{\Omega}_{2a}^2 = \beta^{-1}\Omega^2 - K^2$. The first coefficient is

$$a_0 = \frac{\alpha}{4\beta(\alpha - \beta)}\Omega^4 - (1 + K^2)\Omega^2 + K^2, \tag{3.19}$$

which gives the leading-order approximation a_0=0 to the dispersion relation. In deriving a_0 we have used the identity $\beta(3\alpha - 4\beta)/(\alpha - \beta) = 1$, which follows from the definitions of c_1 and c_2 in terms of Poisson's ratio, as given in (2.2).

The equation $a_0 = 0$ is the membrane-theory approximation [2] to the dispersion relation, in which the bending stiffness of the tube wall is ignored. The higher coefficients a_{2l} contain even powers $K^{2\sigma}\Omega^{2\tau}$ up to $\sigma + \tau = l + 2$, with $\sigma \geq 0$ and $\tau \geq 0$, but excluding $\sigma = \tau = 0$; thus a_{2l} for $l \geq 1$ contains $(l + 2)(l + 5)/2$ terms. Hence a_2 has 9 terms, and a_4 has 14. These numbers of terms are one less than triangular numbers; for $l = 0$ the number is two less, because both K^4 and the constant term are absent.

The second coefficient a_2 in (3.18) may be written $\sum_0^3 a_{2,2\tau}\Omega^{2\tau}$, where

$$a_{20} = \frac{\alpha K^2(-3 + 2K^2) + 2\beta(\alpha - \beta)K^6}{6\alpha}, \tag{3.20}$$

$$a_{22} = \frac{\alpha^2(6 - K^2 - 8K^4) - \alpha\beta(6 + 5K^2 - 12K^4) + 4\beta^2K^2(2 - K^2)}{12\alpha(\alpha - \beta)}, \tag{3.21}$$

$$a_{24} = \frac{\alpha^2(-3 + 16K^2) + 8\alpha\beta(1 - K^2) - 4\beta^2(2 + K^2)}{48\alpha\beta(\alpha - \beta)} \tag{3.22}$$

and

$$a_{26} = -\frac{\alpha + \beta}{24\beta^2(\alpha - \beta)}. \tag{3.23}$$

Here the terms are grouped in powers of (α, β), rather than (Ω, K).

The third coefficient a_4 in (3.18) has the form $\sum_0^4 a_{4,2\tau}\Omega^{2\tau}$, in which $a_{4,2\tau}$ is a polynomial in K of degree $8 - 2\tau$, containing even powers of K only, but we shall need only the highest degree terms in this expression. Their sum is $\tilde{a}_4 = \sum \tilde{a}_{2\sigma,2\tau}K^{2\sigma}\Omega^{2\tau}$, where $\sigma + \tau = 4$ and

$$\tilde{a}_{80} = \frac{2\beta(\alpha - \beta)}{45\alpha}, \quad \tilde{a}_{62} = \frac{-5\alpha^2 + 2\alpha\beta + \beta^2}{45\alpha^2}, \quad \tilde{a}_{44} = \frac{8\alpha^3 - 4\alpha^2\beta - 5\alpha\beta^2 + 2\beta^3}{90\alpha^2\beta(\alpha - \beta)} \tag{3.24}$$

and

$$\tilde{a}_{26} = \frac{-9\alpha^3 - 9\alpha^2\beta + 9\alpha\beta^2 + \beta^3}{360\alpha^2\beta^2(\alpha - \beta)}, \quad \tilde{a}_{08} = \frac{(3\alpha + \beta)(\alpha + 3\beta)}{1440\alpha\beta^3(\alpha - \beta)}. \tag{3.25}$$

Downloaded from https://royalsocietypublishing.org/ on 09 June 2021

4. Elementary theory for a thin-walled tube

Truncations of the series (3.18) give accurate approximations to the exact dispersion relation (3.1). For example, if terms up to order ϵ^4 are retained, the result is accurate up to very high frequencies and wavenumbers even for a thick-walled tube; and if only the first term a_0 is retained, this still provides a good approximation up to $(\Omega, K) = (1, 1)$. Intermediate approximations are also available. These remarks are amplified in what follows, based on numerical evaluation of the exact dispersion relation and its various approximations.

(a) Leading-order terms

The leading-order approximation $a_0 = 0$ is curve a in figure 1, which is for Poisson's ratio $\nu = 0.3$ and dimensionless thickness $\epsilon = 0.25$. This approximation has two branches, and from the identity $4\beta(\alpha - \beta)/\alpha = 1/(1 - \nu^2)$ we may write its equation $a_0 = 0$, except when $\Omega^2 = 1$, in the form

$$\frac{K^2}{1-\nu^2} = \Omega^2 \left\{ \frac{\Omega^2 - (1-\nu^2)^{-1}}{\Omega^2 - 1} \right\}. \tag{4.1}$$

Thus unless $\nu = 0$, the approximation $a_0 = 0$ gives a frequency gap in the range

$$1 < \Omega^2 < \frac{1}{1-\nu^2}, \tag{4.2}$$

for which there are no real values of K. (We treat the case $\nu = 0$ in detail in §5.) In the exact dispersion relation, this gap exists up to K somewhat greater than 1, beyond which the first branch bends over to the right, a feature not captured by the approximation $a_0 = 0$. The steeply rising part of the dispersion curve at and just above $K = 1$ is evident in all the curves in figure 1, and corresponds to a (frequency, wavenumber) region of low group velocity. At first sight, the two parts of curve a with slopes near 1 appear to be close to two parts of a straight line. However, (4.1) shows that the two parts have different slopes, since $\Omega^2 \simeq K^2$ near the origin, but $\Omega^2 \simeq K^2/(1-\nu^2)$ on the other branch. Hence the two parts are not asymptotes to the same straight line unless $\nu = 0$.

The curve a as a whole in figure 1 provides an accurate approximation to the first two branches of the exact dispersion relation, except beyond $\Omega = 1$ on the first branch and except at very high frequencies on the second branch. It is accurate where bending stiffness is negligible, i.e. where membrane theory applies. On the part of curve a with slope close to 1, the displacement is axial, and on the part with nearly vertical slope near the frequency axis, the displacement is radial. The equation $a_0 = 0$ gives a second-branch cut-on frequency $\Omega_0 = (1-\nu^2)^{-1/2}$, which is a first approximation to the ring frequency when $\epsilon \neq 0$, but is exact when $\epsilon = 0$. Nearby, the series expansion of curve a, obtainable from (3.19) or (4.1), is

$$\Omega^2 = \frac{1}{1-\nu^2} + \frac{\nu^2}{1-\nu^2} \left\{ K^2 + (1-\nu^2)K^4 + O(K^6) \right\}. \tag{4.3}$$

The smallness of the coefficient $\nu^2/(1-\nu^2)$ explains the flatness of the dispersion curve near cut-on; for Poisson's ratio $\nu = 0.3$, the value of this coefficient is 0.09890, and in the corresponding expansion of Ω rather than Ω^2, the coefficient of K^2 is 0.04717. These formulae are of course approximations to the exact values, though very good ones, because they are based solely on a_0.

(b) Higher order terms

In (3.18), let us now keep the three terms displayed, except that in a_4 we retain only the highest powers of Ω and K as defined by the coefficients (3.24)–(3.25). The reason for omitting the lower powers is that the term $a_4\epsilon^4$ is significant only at very high frequencies and wavenumbers, and then the lower powers of Ω and K in a_4 may be ignored. In effect, this gives a matching rule to

Downloaded from https://royalsocietypublishing.org/ on 09 June 2021

high frequencies and wavenumbers. The result is the high-order approximation

$$a_0 + a_2\epsilon^2 + \tilde{a}_4\epsilon^4 = 0, \tag{4.4}$$

with a_0 and a_2 given by (3.19)–(3.23), and $\tilde{a}_4$ as defined just before (3.24).

Numerical evaluation shows that approximation (4.4) is spectacularly accurate. In figure 1, for $\nu = 0.3, \epsilon = 0.25$, it gives branches b which are almost indistinguishable from the exact branches up to $\Omega = 9$ and $K = 10$. Even for ϵ as large as 0.5, corresponding to a tube with outer radius three times the inner radius, the curves are indistinguishable up to $\Omega = 4$ and $K = 6$. Thus the approximation applies even for a thick-walled tube up to high frequencies and wavenumbers.

(c) Dispersion relation near the ring frequency

Near the ring frequency, the approximation (4.3) may be extended to include as many terms $b_{2n,2m}\epsilon^{2n}K^{2m}$ as desired, where the coefficients $b_{2n,2m}$ may be calculated exactly from (3.18) as rational expressions in α and β, or equivalently in ν from (2.2). The displayed terms in (4.3) correspond to

$$b_{00} = \frac{1}{1-\nu^2}, \quad b_{02} = \frac{\nu^2}{1-\nu^2} \quad \text{and} \quad b_{04} = \nu^2, \tag{4.5}$$

and beyond this the simplest coefficients are

$$b_{20} = \frac{\beta(\alpha-\beta)(5\alpha-8\beta)}{3\alpha^2} = \frac{1+3\nu}{12(1-\nu^2)(1-\nu)} = \frac{1}{12} + \frac{\nu}{3} + \frac{5\nu^2}{12} + \frac{2\nu^3}{3} + \cdots \tag{4.6}$$

and

$$b_{22} = -\frac{2\beta(\alpha^3 - 2\alpha^2\beta + 2\alpha\beta^2 - 2\beta^3)}{3\alpha^3} = -\frac{1-4\nu^2(1-\nu)}{12(1-\nu^2)(1-\nu)^2} = -\frac{1}{12} - \frac{\nu}{6} - \frac{\nu^3}{6} - \frac{\nu^4}{12} + \cdots. \tag{4.7}$$

Here the series form of b_{22} has no term in ν^2.

Instead of using exact expressions for $b_{2n,2m}$, an alternative is to use the coupling theory developed in §5, with Poisson's ratio regarded as a small parameter at the outset. Full details are given in §6.

(d) Intermediate approximations

We saw that on the first branch of the dispersion relation, the approximation $a_0 = 0$ is valid up to near $\Omega = 1$. To go beyond this in the simplest way, i.e. using as few terms as possible from the approximation (4.4), we use the method of dominant balances, in which scalings of Ω and K in powers of ϵ are identified for which a number of terms balance at leading order, the remaining terms all being smaller as measured by the power of ϵ they contain.

The first such balance is $\Omega = 1 + O(\epsilon^{2/3})$, $K = O(\epsilon^{-1/3})$, which brings in the term of order K^6 from a_2, to be added to the terms in a_0. The result is the approximation

$$\frac{\alpha}{4\beta(\alpha-\beta)}\Omega^4 - (1+K^2)\Omega^2 + K^2 + \epsilon^2\frac{\beta(\alpha-\beta)}{3\alpha}K^6 = 0, \tag{4.8}$$

plotted as curve c in figure 1 for $\nu = 0.3, \epsilon = 0.25$. This approximation corrects the asymptote in a_0, and is accurate up to about $K = 3$ on the first branch, and $K = 4$ on the second branch. Equation (4.8) is practical, as it captures in the simplest way the transition which occurs as Ω increases through 1.

The next balance is $\Omega = O(1)$, $K = O(\epsilon^{-1/2})$, but with Ω not too close to 1 (in which case the previous balance would apply). The leading terms, of order ϵ^{-1}, give a subset of the terms in (4.8), and so do not give a new result. Inclusion of the next highest terms, of order 1, gives the

Downloaded from https://royalsocietypublishing.org/ on 09 June 2021

approximation

$$a_0 + \hat{a}_2\epsilon^2 + \hat{a}_4\epsilon^4 = 0, \tag{4.9}$$

where

$$\hat{a}_2 = \frac{\beta(\alpha-\beta)K^6 + \{(\beta-2\alpha)\Omega^2 + \alpha\}K^4}{3\alpha}, \quad \hat{a}_4 = \frac{2\beta(\alpha-\beta)K^8}{45\alpha}. \tag{4.10}$$

Curve d in figure 1 shows that on the upper branch this is accurate up to about $\Omega = 4$, $K = 8$ for $\nu = 0.3$, $\epsilon = 0.25$, extending the range of (4.8). Our starting point for this balance, $K = O(\epsilon^{-1/2})$, is targeting the upper branch fairly high up, and so high accuracy of (4.9) is not to be expected on the lower branch. Nevertheless, the figure shows that accuracy is maintained up to about $K = 2$, and the approximation is at least qualitatively correct on the lower branch up to about $K = 4$. Similar remarks apply, but with less force, to the previous approximation for $K = O(\epsilon^{-1/3})$, because $\epsilon^{-1/3} \ll \epsilon^{-1/2}$ when $\epsilon \ll 1$, so that the target area is then lower; and indeed, curve c is more accurate than curve d on the lower branch, but less accurate on the upper branch.

Other approximations, based on subsets of the terms in (4.4), are possible. These involve a trade-off between accuracy in different regions. We have presented only approximations with no spurious branches, but in fact there are outstanding approximations whose only flaw is a spurious branch. The most notable of these is the approximation $a_0 + a_2\epsilon^2 = 0$, keeping the terms up to order ϵ^2, but no others. This is nearly as accurate as (4.4), but has a spurious branch to the left of the third branch in figure 1, and of a similar shape. The absence of spurious branches is an advantage in practice, and we have found that matching to high frequencies, by the inclusion of selected higher terms, such as $\tilde{a}_4\epsilon^4$, eliminates them. We regard high-frequency matching, based on rational scaling arguments of the type presented here, to be an invaluable part of the theory.

5. Factorization and coupling theory

When Poisson's ratio is zero, the dispersion relation (3.1) contains a factor $\Omega^2 - K^2$. This is an exact result for any thickness of the tube wall, not dependent on series expansions in ϵ. Geometrically, it means that the straight line pair $\Omega^2 = K^2$ crosses other branches of the dispersion curve. Dynamically, the explanation is that, for zero Poisson's ratio, an axially propagating compression wave (a 'bar wave') is decoupled from any other type of wave motion in the tube, because it produces no lateral displacement. Since the dispersion relation of this wave is $\Omega^2 - K^2 = 0$, the factorization property follows at once.

Henceforth, Poisson's ratio ν is taken to be a small parameter. In view of the identities

$$\nu = \frac{\alpha - 2\beta}{2(\alpha-\beta)}, \quad 1 - \nu^2 = \frac{\alpha}{4\beta(\alpha-\beta)}, \tag{5.1}$$

it follows that equivalent criteria to $\nu = 0$ for factorization, i.e. for decoupling, are $\alpha = 2\beta$ or $4\beta(\alpha-\beta)/\alpha = 1$.

The factorization might be thought to be too special to be of interest, as it occurs for only one value of ν. But numerical results show that, for any value of ν in the allowed range $-1 \leqslant \nu \leqslant \frac{1}{2}$, the first two branches of the dispersion relation are merely perturbed versions of the factorized form for $\nu = 0$. For example, in figure 1, for Poisson's ratio 0.3, the narrow waist near $(\Omega, K) = (1, 1)$ is an avoided crossing (veering) [13] between a curve close to the straight line $\Omega = K$ and another curve proceeding upwards and then to the right. That is, the waist is recognizably a perturbation of a crossing. This suggests that a perturbation analysis for small ν, i.e. weak coupling, will give accurate results in a wide range about zero, i.e. for Poisson's ratios which are not in fact small and the coupling is quite strong. In this second half of the paper, we provide such an analysis, and demonstrate numerically the high accuracy of the resulting perturbation series.

(a) A coupling ansatz

To obtain an ansatz representing the type and strength of coupling, it is simplest to start by expanding the coefficients $a_0, a_2, a_4 \ldots$ in (3.18) in powers of ν, using the definitions $\alpha = (c_1/c_0)^2$

Downloaded from https://royalsocietypublishing.org/ on 09 June 2021

and $\beta = (c_2/c_0)^2$. This gives

$$a_0 = (\Omega^2 - K^2)(\Omega^2 - 1) - \nu^2\Omega^4, \tag{5.2}$$

$$a_2 = (\Omega^2 - K^2)(p_{20} + \nu p_{21}) - \nu^2(q_{20} + \nu q_{21} + \nu^2 q_{22} + \cdots) \tag{5.3}$$

and

$$a_4 = (\Omega^2 - K^2)(p_{40} + \nu p_{41}) - \nu^2(q_{40} + \nu q_{41} + \nu^2 q_{42} + \cdots), \tag{5.4}$$

and so on, where the quantities p_{mn} and q_{mn} are polynomials in Ω^2 and K^2. The key feature here, which is not obvious in advance, is that every term of order ν^0 and ν^1 is divisible by $\Omega^2 - K^2$. Hence rearrangement of the terms in (3.18) gives

$$\begin{aligned}(\Omega^2 - K^2)\{\Omega^2 - 1 + \epsilon^2(p_{20} + \nu p_{21}) + \epsilon^4(p_{40} + \nu p_{41}) + \cdots\}\\ = \nu^2\{\Omega^4 + \sum_{n=0}^{\infty} \nu^n(\epsilon^2 q_{2,n} + \epsilon^4 q_{4,n} + \cdots)\},\end{aligned} \tag{5.5}$$

which we shall call the coupling ansatz form of the dispersion relation. The right-hand side gives an exact measure of the coupling which occurs when ν is perturbed from the special value $\nu = 0$ at which coupling is absent. In this latter case, the dispersion relation separates into $\Omega^2 = K^2$ and

$$\Omega^2 - 1 + \epsilon^2 p_{20} + \epsilon^4 p_{40} + \cdots = 0. \tag{5.6}$$

Thus when $\nu = 0$, crossings occur when (5.6) and the equation $\Omega^2 = K^2$ hold simultaneously. The crossing points may be written $(\Omega, K) = (\Omega_c(\epsilon), K_c(\epsilon))$, and in §8 we give an expression for the first crossing point, which is close to $(\Omega, K) = (1, 1)$. Another special value is $\epsilon = 0$, for which (5.5) reduces to $a_0 = 0$. By (5.2), this is a quadratic equation in Ω^2, with roots

$$\Omega^2 = \frac{1 + K^2 \pm \{(1 - K^2)^2 + 4\nu^2 K^2\}^{1/2}}{2(1 - \nu^2)}. \tag{5.7}$$

When $K = 0$, this gives $\Omega^2 = 0$ and $\Omega^2 = 1/(1 - \nu^2)$, the latter giving an exact expression for the ring frequency when $\epsilon = 0$, consistent with §4a and the value of b_{00} given in (4.5).

The coefficients in (5.5) are found by expanding the formulae in §3c in powers of ν. The first few are

$$p_{20} = \frac{1}{12}\{6 - (\Omega^2 + 4K^2) - (2\Omega^2 - K^2)(3\Omega^2 - K^2)\}, \quad p_{21} = -\frac{1}{6}\Omega^2(2\Omega^2 - K^2) \tag{5.8}$$

and

$$q_{20} = \frac{1}{12}\{\Omega^2(\Omega^2 - 4K^2) - (10\Omega^6 - 6\Omega^4 K^2 - 2\Omega^2 K^4 + K^6)\}. \tag{5.9}$$

(b) A hierarchy of approximations

To construct approximations which are accurate over a wide range, we again use the method of dominant balances, in which as many terms as possible in an equation are balanced at leading order [10,11,15]. Numerically, it is found that the resulting approximations are accurate over a wider range than is implied by the assumptions. In (5.5), a dominant balance is achieved by taking Ω and K to be of order 1, and ϵ and ν to be small quantities of the same order of magnitude.

In this way, we obtain a hierarchy of approximations $D_0, D_2, \ldots$ to the dispersion relation (5.5). The first approximation D_0 contains only the leading-order terms, and is the factorized form

$$(\Omega^2 - K^2)(\Omega^2 - 1) = 0. \tag{5.10}$$

The next approximation D_2 includes also the terms in ϵ^2 and ν^2, and so is

$$(\Omega^2 - K^2)(\Omega^2 - 1 + \epsilon^2 p_{20}) = \nu^2\Omega^4. \tag{5.11}$$

To construct D_4, we could include the terms in $\nu\epsilon^2$, ϵ^4 and $\nu^2\epsilon^2$. (There are no terms of order ν^n for $n > 2$ in truncations of (5.5), because the exact expression (5.2) for a_0 terminates at order ν^2.) However, as in §4b, it is sufficient to retain in p_{40} and q_{20} only the highest powers of Ω and K,

Downloaded from https://royalsocietypublishing.org/ on 09 June 2021

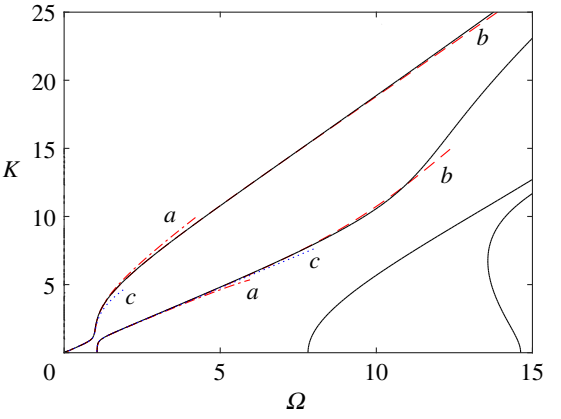

Figure 2. Factorized-form approximations to the dispersion relation for Poisson's ratio $\nu = 0.3$ and thickness $\epsilon = 0.25$. The approximations and their equation numbers are (*a*) (red, dash-dotted): (5.11); (*b*) (red, dashed): (5.12); (*c*) (blue, dotted): (5.13). Exact dispersion curves from (3.1) are black, solid. As in figure 1, the placings of the letters indicate the range of validity of the approximations. Curve (*c*) is also shown as curve (*e*) in figure 1. (Online version in colour.)

since this suffices to give excellent matching when Ω and K approach values of order ϵ^{-1}. These powers are the terms of degree 6 in p_{40} and q_{20}, which we denote p_{406} and q_{206}. Therefore, we take approximation D_4 to be

$$(\Omega^2 - K^2)\{\Omega^2 - 1 + \epsilon^2(p_{20} + \nu p_{21}) + \epsilon^4 p_{406}\} = \nu^2(\Omega^4 + \epsilon^2 q_{206}). \tag{5.12}$$

The Novozhilov–Goldenvizer and Donnell–Mushtari approximation in shell theory [2,16] is

$$(\Omega^2 - K^2)(\Omega^2 - 1 - \frac{1}{12}\epsilon^2 K^4) = \nu^2\Big\{\Omega^4 - \frac{\epsilon^2 K^6}{12(1-\nu^2)}\Big\}. \tag{5.13}$$

This is similar in form to (5.12) with suitable coefficients, especially p_{21} and p_{406} taken to be zero, except that q_{206} now depends also on ν.

Approximations D_2 and D_4 are shown as curves *a* and *b* in figure 2 for $(\nu, \epsilon) = (0.3, 0.25)$. Their wide range of accuracy is evident, and D_4 in particular extends the frequency and wavenumber range of the shell theory approximation (5.13), marked as curve *c*. See also figure 1, which includes (5.13) as curve *e*. A comparison of figures 1 and 2 shows that, numerically, nothing is lost by using low-order series in Poisson's ratio, as opposed to the corresponding exact expressions. Functionally, much is gained, because of the clarity of (5.10)–(5.12).

6. The ring frequency and negative group velocity

We now determine the shape of the dispersion curve at frequencies near the ring frequency, i.e. near the cut-on frequency of the second branch. Our method is to obtain a series expansion for Ω^2 as a function of K^2 in a wide range of K at frequencies near cut-on, using the coupling theory just developed. This approach is simpler than using the exact formulae of §4, and gives approximations which numerically are almost indistinguishable from exact results. The main result is that for a range of values of Poisson's ratio, the width of which depends on the thickness of the tube wall, there is a region of negative group velocity, i.e. an arc of the dispersion curve which slopes backwards at frequencies just below the ring frequency. Although such arcs are known to occur in related problems, e.g. for symmetric waves in a plane layer [17,18] and non-axisymmetric waves in a fluid-loaded tube [19], this is a new result for axisymmetric waves or an unloaded tube. We verify it below, both from the exact dispersion relation (3.1) and from a coupling expansion, which describes it in fine detail.

Downloaded from https://royalsocietypublishing.org/ on 09 June 2021

(a) Ansatz for the cut-on region

A suitable ansatz for the dispersion curve near the cut-on region is

$$\Omega^2 = 1 + A_{02}\nu^2 + A_{04}\nu^4 + \ldots + \sum_{n=0}^{\infty} \nu^n(\epsilon^2 A_{2,n} + \epsilon^4 A_{4,n} + \cdots), \tag{6.1}$$

where the coefficients A_{mn} are functions of K^2. Here only even powers of ν occur in the ϵ^0 terms, but both odd and even powers of ν multiply the powers $\epsilon^2, \epsilon^4, \ldots$. Substitution of (6.1) into the dispersion relation (3.18) gives

$$A_{02} = \frac{1}{1-K^2}, \quad A_{04} = \frac{1-2K^2}{(1-K^2)^3}, \quad A_{20} = \frac{1}{12}\{1 - K^2(1-K^2)\}, \quad A_{21} = \frac{1}{3}\left(1 - \frac{1}{2}K^2\right), \tag{6.2}$$

and further terms are readily obtained. Asymmetry in Poisson's ratio first occurs in terms of order $\nu\epsilon^2$, via A_{21}, and next in terms of order $\nu^3\epsilon^2$ and $\nu\epsilon^4$.

A check of the ϵ^0 terms in (6.1) is that they agree with the Taylor series expansion in ν of the exact result (5.7), with the positive sign before the square root. The coefficients (6.2) are exact, i.e. they are not simply leading-order approximations to more accurate expressions. They show that the square of the ring frequency, obtained from (6.1) evaluated at $K = 0$, is

$$\Omega^2 = \frac{1}{1-\nu^2} + \epsilon^2\left(\frac{1}{12} + \frac{\nu}{3} + \frac{5\nu^2}{12} + \frac{2\nu^3}{3} + \cdots\right) - \epsilon^4\left(\frac{1}{48} - \frac{11\nu}{180} + \cdots\right) + O(\nu^4\epsilon^2, \nu^2\epsilon^4, \epsilon^6). \tag{6.3}$$

Here, the terms multiplying ϵ^2 agree with (4.6), i.e. the exact expression in α and β for b_{20}. The terms multiplying ϵ^4 would be obtainable from a lengthy expression for b_{40} if the coupling approach were not used.

For non-zero K, we again adopt a dominant balance approach by selecting the leading terms when ϵ and ν are assumed to be small but of the same order. This gives

$$\Omega^2 = 1 + \frac{\nu^2}{1-K^2} + \frac{\epsilon^2}{12}\{1 - K^2(1-K^2)\} + \frac{\nu\epsilon^2}{3}\left(1 - \frac{1}{2}K^2\right) + O(\nu^4, \nu^2\epsilon^2, \epsilon^4), \tag{6.4}$$

in which the functions of K are exact. However, we have the option of expanding these functions in powers of K, if $K^2 < 1$. This gives, to third order,

$$\Omega^2 = 1 + \nu^2 + \frac{\epsilon^2}{12} + \frac{\nu\epsilon^2}{3} + \left(\nu^2 - \frac{\epsilon^2}{12} - \frac{\nu\epsilon^2}{6}\right)K^2 + \left(\nu^2 + \frac{\epsilon^2}{12}\right)K^4 + O(\nu^4, \nu^2\epsilon^2, \epsilon^4, \nu^2K^6). \tag{6.5}$$

When $K = 0$, this agrees with (6.3) to the order stated. The coefficient of K^4 in (6.5) has no term of order $\nu\epsilon^2$ because the exact expression for A_{21} in (6.2) is quadratic in K; it also has no terms of order ν^n for $n > 2$, a consequence of the exact expression for b_{04} in (4.5). A short calculation shows that the fourth-order terms in the coefficient of K^2 are $\nu^4 - \epsilon^4/60$, but there is no term in $\nu^2\epsilon^2$. It is not easy to see in advance which terms will be absent.

(b) Region of negative group velocity near the ring frequency

A striking feature of (6.5) is that the coefficient of K^2 is negative when $\nu^2/(1+2\nu) < \epsilon^2/12$. This condition is equivalent to $\nu_-(\epsilon) < \nu < \nu_+(\epsilon)$ where

$$\nu_\pm(\epsilon) = \pm\frac{\epsilon}{\sqrt{12}} + \frac{\epsilon^2}{12} + O(\epsilon^3). \tag{6.6}$$

Thus for Poisson's ratios which are not too large in modulus, the dispersion curve slopes backwards near the ring frequency, corresponding to negative group velocity. This is the new result referred to earlier. In particular, the slope is always backwards when Poisson's ratio is zero. We have seen in figures 1 and 2 that approximations based on series in ϵ^2 are accurate when ϵ is as large as 0.25, and further numerical calculations have confirmed their accuracy up to ϵ somewhat beyond 0.4. Thus a region of negative group velocity near cut-on is confirmed to exist in a large region of (ϵ, ν) parameter space. Only for extremely thin-walled tubes, i.e. very small ϵ, is the

Downloaded from https://royalsocietypublishing.org/ on 09 June 2021

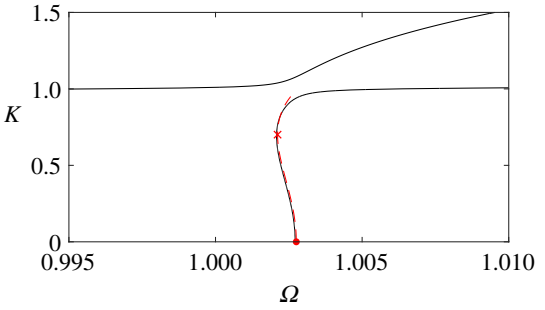

Figure 3. Region of negative group velocity (backward slope) for $(\epsilon, \nu) = (0.25, 0.01)$. The solid curves are parts of the first and second branches of the exact dispersion relation (3.1), and the red dashed curve is approximation (6.5). The dot is at the ring frequency, where $K = 0$, and the cross is at the critical point, where $(\Omega, K) = (\Omega_\mathrm{m}, K_\mathrm{m})$; these lie on the dashed curve. Note the elongated frequency scale: the arc of negative group velocity would be indistinguishable from a vertical straight line if drawn on the scale of figures 1 or 2, and the two branches would appear to join up and cross. (Online version in colour.)

existence of the region restricted to a narrow range of Poisson's ratio. From (6.6), the asymmetry of the region is evident: it extends slightly further to positive ν than to negative ν.

Differentiation of (6.5) shows that $\mathrm{d}\Omega/\mathrm{d}K = 0$ at the critical wavenumber $K = K_\mathrm{m} = K_\mathrm{m}(\epsilon, \nu)$, where

$$K_\mathrm{m}^2 \simeq \frac{1}{2}\left(\frac{1 + 2\nu - 12\nu^2/\epsilon^2}{1 + 12\nu^2/\epsilon^2}\right). \tag{6.7}$$

The frequency has a local minimum $\Omega = \Omega_\mathrm{m}$ at this wavenumber. A check of the neglected terms in (6.5), notably the term $O(\nu^2 K^6)$, shows that approximation (6.7) is valid when either $K_\mathrm{m} \ll 1$ or $|\nu| \ll \epsilon$. The former case arises for $\nu \simeq \nu_\pm(\epsilon)$, and the latter for $K_\mathrm{m} \simeq 1/\sqrt{2}$. The range of negative group velocity is $0 < K < K_\mathrm{m}$. Since K_m is of order one except when ν is very close to $\nu_\pm(\epsilon)$, it follows that this wavenumber range is broad in general.

Formulae (6.1)–(6.7) simplify when Poisson's ratio is zero, because so many of the terms then vanish. A full parameter study in the (ϵ, ν) plane requires the exact expressions (6.2), rather than the series approximation in K used in (6.5), and will be reported elsewhere. Figure 3 shows the region of negative group velocity in the (Ω, K) plane for $(\epsilon, \nu) = (0.25, 0.01)$. The solid curves are exact, as calculated from (3.1), and the dashed curve is approximation (6.5). It can be seen that the agreement is excellent. The arc of negative group velocity extends from the ring frequency, marked with a dot, to the critical point, marked with a cross. These points are obtained from (6.5) evaluated at $K = 0$ for the ring frequency, and at $(\Omega, K) = (\Omega_\mathrm{m}, K_\mathrm{m})$ for the critical point.

The horizontal scale of the figure shows that the frequency is almost constant over a wide range of wavenumbers. Physically, this means that, near the ring frequency, a wide range of axial wavenumbers can be excited simultaneously, making possible a localized field which may need a nonlinear correction in order to be represented accurately [20,21]. This is even more pronounced when $\nu = \nu_\pm(\epsilon)$, because the coefficient of K^2 in (6.5) is then zero, and the dispersion curve becomes even flatter near the ring frequency, having a quartic form in K rather than its usual parabolic form. The extra flatness for $\nu = \nu_\pm(\epsilon)$ is yet further enhanced by the smallness of the coefficient of K^4, which is then only $\epsilon^2/6 + O(\epsilon^4)$, with the result that Ω^2 differs from a constant by only $\epsilon^2 K^4/6$, to leading order.

The region of negative group velocity is not captured by thin shell approximations, for example (5.13). The formulae above suggest that a suitable form of thick shell theory is required, designed to be uniformly accurate in a whole neighbourhood of $(\epsilon, \nu) = (0, 0)$ in parameter space, rather than merely in the 'outer limit' $\epsilon \to 0$ at fixed ν. Such a development could be useful in the theory of metamaterials designed to have small or negative Poisson's ratio, and also in the theory of

Downloaded from https://royalsocietypublishing.org/ on 09 June 2021

nanotubes [20,21]. A possible starting point would be to include transverse shear and rotational inertia, as in [22], for example.

7. The modified bar wave

We now determine how the bar wave dispersion relation $\Omega^2 = K^2$ must be modified to take account of non-zero Poisson's ratio ν. Analysis of (5.5) reveals that a suitable ansatz is

$$\Omega^2 = K^2 + \nu^2 K^4 \Big\{ B_{00} + \nu^2 B_{02} + \cdots + \sum_{n=0}^{\infty} \nu^n (\epsilon^2 B_{2,n} + \epsilon^4 B_{4,n} + \cdots) \Big\}, \tag{7.1}$$

where the coefficients B_{mn} are functions of K^2. Only even powers of ν occur in the ϵ^0 terms, and positive powers of ϵ are multiplied by at least ν^2. Substitution of (7.1) into (5.5) gives

$$B_{00} = \frac{-1}{1-K^2}, \quad B_{02} = \frac{K^2(2-K^2)}{(1-K^2)^3}, \quad B_{20} = \frac{-3+5K^2-K^4}{12(1-K^2)^2} \quad \text{and} \quad B_{21} = \frac{K^2(2-K^2)}{6(1-K^2)^2}, \tag{7.2}$$

and so on. The terms of (7.1) up to fourth order in ϵ and ν are

$$\Omega^2 = K^2 + \nu^2 K^4 (B_{00} + \epsilon^2 B_{20} + \nu^2 B_{02}) + O(\nu^2\epsilon^4, \nu^3\epsilon^2, \nu^6), \tag{7.3}$$

and expansion of the exact coefficients (7.2) in powers of K for $K^2 < 1$, followed by ordering in powers of K, gives

$$\Omega^2 = K^2 - \nu^2 K^4 \Big(1 + \frac{1}{4}\epsilon^2\Big) - \nu^2 K^6 \Big(1 - 2\nu^2 + \frac{1}{12}\epsilon^2 - \frac{1}{3}\nu\epsilon^2 + \cdots\Big) + \cdots. \tag{7.4}$$

Here, the coefficients of K^2 and K^4 are exact, and the omitted terms in the coefficient of K^6 are $O(\nu^2\epsilon^4, \nu^4\epsilon^2, \nu^6)$. The coefficient of K^8 is $O(\nu^2)$.

The series (7.4) converges when $K^2 < 1$, but increasingly slowly as the waist region near $(\Omega, K) = (1, 1)$ is approached. This region admits a separate analysis, which we now provide.

8. The waist region

(a) Exact crossing

When $\nu = 0$ the bar wave dispersion curve $\Omega^2 = K^2$ crosses the branch (5.6) near the point $(\Omega, K) = (1, 1)$. The coordinates $(\Omega_c(\epsilon), K_c(\epsilon))$ of this point may be found as a series in ϵ^2 by taking $\Omega = K$ in (5.6), which gives

$$\Omega_c^2(\epsilon) = K_c^2(\epsilon) = 1 + \frac{1}{12}\epsilon^2 - \frac{1}{48}\epsilon^4 + \cdots. \tag{8.1}$$

A check here is that (8.1) is the same as expansion (6.3) for the ring frequency when $\nu = 0$. Recall the exact result, established in §3, that for Poisson's ratio of zero, the crossing frequency and the ring frequency are the same, a consequence of the block structure of the exact determinant (3.1).

(b) Avoided crossing

To determine how the crossing is avoided when $\nu \neq 0$, in accordance with veering theory [13], it is simplest to define local variables (ξ, η) by

$$\Omega^2 = \Omega_c^2(\epsilon) + \xi, \quad K^2 = K_c^2(\epsilon) + \xi + \eta, \tag{8.2}$$

and substitute into (5.5). On retaining all terms up to $O(\epsilon^2, \nu^2)$, while allowing ξ and η to be as large as order one, we obtain

$$\eta \Big\{ \xi - \frac{1}{12}\epsilon^2 \big[9\xi + \eta + (\xi - \eta)(2\xi - \eta)\big] \Big\} + \nu^2 (1+\xi)^2 = 0, \tag{8.3}$$

Downloaded from https://royalsocietypublishing.org/ on 09 June 2021

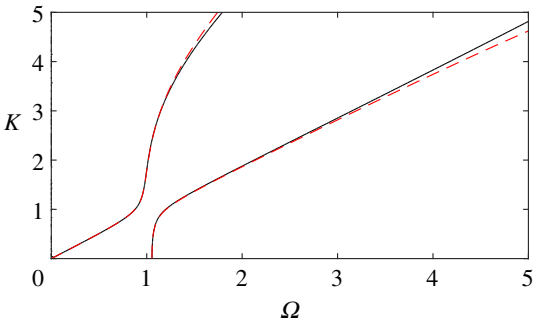

Figure 4. Approximation based on local variables centred on $(\Omega, K) = (\Omega_c(\epsilon), K_c(\epsilon))$, near (1, 1), for $(\epsilon, \nu) = (0.25, 0.3)$. The solid curves are from the exact dispersion relation (3.1), and the red dashed curves are approximation (8.3). (Online version in colour.)

with error of $O(\epsilon^2\nu, \epsilon^4)$. There are no error terms here of order ν^n, for any n, because (8.3) is exact when $\epsilon = 0$; it is then the equation $a_0 = 0$ expressed in different variables, where a_0 first appeared in (3.18) and has reappeared in different guises since then.

Approximation (8.3) is accurate over a wide range, as may be seen in figure 4, for $(\epsilon, \nu) = (0.25, 0.3)$. In constructing the figure, ξ and η are expressed in terms of $(\Omega^2, K^2, \epsilon)$ using (8.2), but with (8.1) truncated to $1 + \epsilon^2/12$, because (8.3) is defined to exclude terms of order ϵ^4. The accuracy extends down to $K = 0$ as well as up to $\Omega \simeq 5$ and $K \simeq 5$, even though both ν and ϵ are far from small. The reasons for this wide range of applicability of (8.3) are twofold: (i) the expansion is about the most degenerate point, namely $(\Omega, K) = (\Omega_c(\epsilon), K_c(\epsilon))$, which acts as an organizing centre in the sense of bifurcation theory [23,24]; and (ii) the method of dominant balances has been used in choosing the scalings to retain as many terms as possible at the same order of magnitude, here $\epsilon \sim \nu \ll 1$ and $\xi \sim \eta \sim O(1)$ in the terms after the leading approximation $\xi\eta = 0$.

9. Conclusion and further work

This paper has exploited a family of Wronskian identities to reduce a transcendental dispersion relation to a series form in which the coefficients are low-order polynomials in the frequency and wavenumber. By this means, a number of accurate approximations to the dispersion relation have been derived, many of them tailored to particular regions of the (frequency, wavenumber) plane and valid beyond the range of thin shell theories. Mathematically, the method of 'higher Wronskians' and their properties offers scope for further use in mathematical science, because it applies to linear boundary-value problems in general. Physically, as noted in §6, new extensions of shell theory may be possible, for example by using the method of dominant balances in an energy functional to determine a distinguished scaling in the shell thickness and Poisson's ratio simultaneously.

Promising applications are to metamaterials and nanotubes [20,21], including extensions to account for transverse shear and rotational inertia [22], and nonlinearity. In particular, the concluding section of [21] is explicit that current shell theory still has unresolved difficulties near the ring frequency, because of the difficulty in framing suitable kinematic hypotheses to account for the near-inextensibility of the mid-surface of the tube wall, and the parabolic form of the even part of the circumferential stress. We see opportunities to combine our methods with those of [20–22] to obtain new results, especially taking account of our comments in §6b about the extreme flatness of the dispersion relation near the ring frequency, and the resulting possibility of localized fields. An important feature of our results is that once the dispersion relation is known to guaranteed accuracy, equations (2.14)–(2.15) then determine all stress, strain, and displacement components explicitly. Hence series expansions of (2.14)–(2.15) in the transverse

Downloaded from https://royalsocietypublishing.org/ on 09 June 2021

coordinate determine unambiguously the dominant shape of cross-layer profiles—an important step in resolving doubts which might be felt about the kinematic hypotheses of shell theory near the ring frequency.

Three new results in particular have emerged during our numerical experimentation with the new formulae we have derived. The first is that for any thickness of the tube wall there exists a range of Poisson's ratio ν for which, near the ring frequency, the group velocity is negative. This range always includes $\nu = 0$, and increases in width as the tube wall becomes thicker. If the wall is not too thick, the range is given by (6.6). It should be noted that a thin shell approach in which Poisson's ratio is held fixed, while the thickness of the tube wall is made arbitrarily small, may not detect negative group velocities, which are not present for a thin enough shell at fixed non-zero Poisson's ratio.

The second new result is that perturbation analyses taking Poisson's ratio to be a small parameter are numerically accurate well beyond their initially assumed range, and extend at least as far as $\nu = \pm 0.3$. This means that the factorization and coupling theory developed from §5 onwards, though superficially restricted in scope compared with the earlier approach, in fact loses nothing—and has the advantage of capturing explicitly the negative group velocity.

The third new result is that simple approximations are accurate up to surprisingly high frequencies and wavenumbers, illustrated for example by the dashed curves b in figure 1. The key feature here is that the main small parameter of the theory is the dimensionless thickness ϵ, and only later do we need to consider possible restrictions on frequency and wavenumber. Numerically, ϵ need not be small. The graphs in the paper are for $\epsilon = 0.25$, and we have found that much of the accuracy is maintained when ϵ is as high as 0.4. Thus the formulae in the paper are valid for a very wide range of thickness, Poisson's ratio, frequency and wavenumber.

Data accessibility. The paper does not report primary data.

Authors' contributions. Both of the authors have contributed substantially to the paper.

Competing interests. We declare we have no competing interests.

Funding. Part of the work was carried out at the Isaac Newton Institute for Mathematical Sciences during the programme 'Complex analysis: techniques, applications and computations', funded by EPSRC grant no. EP/R014604/1. The work was also funded by Keele and Aalborg Universities.

Acknowledgements. The authors thank J. D. Kaplunov at Keele and S. G. Mogilevskaya at the Isaac Newton Institute, Cambridge University, for helpful comments.

References

1. Love AEH. 1944 *A treatise on the mathematical theory of elasticity*, 4th edn. New York, NY: Dover.
2. Novozhilov VV. 1964 *Thin shell theory*, 2nd edn. Groningen, The Netherlands: Noordhoff.
3. Graff KF. 1975 *Wave motion in elastic solids*. New York, NY: Dover.
4. Kang B, Riedel CH, Tan CA. 2003 Free vibration analysis of planar curved beams by wave propagation. *J. Sound Vib.* **260**, 19–44. (doi:10.1016/S0022-460X(02)00898-2)
5. Gazis DC. 1958 Exact analysis of the plane-strain vibrations of thick-walled hollow cylinders. *J. Acoust. Soc. Am.* **30**, 786–794. (doi:10.1121/1.1909761)
6. Chapman CJ, Sorokin SV. 2017 The deferred limit method for long waves in a curved waveguide. *Proc. R. Soc. Lond. A* **473**, 20160900 (doi:10.1098/rspa.2016.0900)
7. Watson GN. 1995 *A treatise on the theory of Bessel functions*. Cambridge, UK: Cambridge University Press.
8. Magnus W, Oberhettinger F, Soni RP. 1966 *Formulas and theorems for the special functions of mathematical physics*, 3rd edn. Berlin, Germany: Springer.
9. Olver FWJ, Lozier DW, Boisvert RF, Clark CW. 2010 *NIST handbook of mathematical functions*. Cambridge, UK: Cambridge University Press.
10. Bender CM, Orszag SA. 1978 *Advanced mathematical methods for scientists and engineers*. New York, NY: McGraw-Hill.
11. Hinch EJ. 1991 *Perturbation methods*. Cambridge, UK: Cambridge University Press. (doi:10.1017/CBO97811 39172189).
12. Lax PD. 1997 *Linear algebra*. New York, NY: Wiley.
13. Mace BR, Manconi E. 2012 Wave motion and dispersion phenomena: veering, locking and strong coupling effects. *J. Acoust. Soc. Am.* **131**, 1015–1028. (doi: 10.1121/1.3672647)

14. Morse PM, Feshbach H. 1953 *Methods of theoretical physics, Part II*. New York, NY: McGraw-Hill.
15. Chapman CJ, Wynn HP. 2021 Fractional power series and the method of dominant balances. *Proc. R. Soc. Lond. A* **477**, 20200646 (doi:10.1098/rspa.2020.0646)
16. Zadeh MN, Sorokin SV. 2013 Comparison of waveguide properties of curved versus straight planar elastic layers. *Mech. Res. Commun.* **47**, 61–68. (doi:10.1016/j.mechrescom.2012.09.003)
17. Mindlin RD. 1955 An introduction to the mathematical theory of vibrations of elastic plates. Signal Corps Engineering Laboratories, Project 142B. Fort Monmouth, NJ.
18. Shuvalov AL, Poncelet O. 2008 On the backward Lamb waves near thickness resonances in anisotropic plates. *Int. J. Solids Struct.* **45**, 3430–3448. (doi:10.1016/j.ijsolstr.2008.02.004)
19. Sorokin SV. 2003 An introduction to the theory of wave propagation in elastic cylindrical shells filled with an acoustic medium. Institute of Machine Acoustics, Project B1, pp. 1–42. Aalborg University, Denmark.
20. Andrianov IV, Kaplunov J, Kudaibergenov AK, Manevitch LI. 2018 The effect of a weak nonlinearity on the lowest cut-off frequencies of a cylindrical shell. *Z. Angew. Math. Phys.* **69**, 1–12. (doi:10.1007/s00033-017-0902-9)
21. Ege N, Erbaş B, Kaplunov J. 2021 Asymptotic derivation of refined dynamic equations for a thin elastic annulus. *Math. Mech. Solids* **26**, 118–132. (doi:10.1177/1081286520944980)
22. Naghdi PM, Cooper RM. 1956 Propagation of elastic waves in cylindrical shells, including the effects of transverse shear and rotatory inertia. *J. Acoust. Soc. Am.* **28**, 56–63. (doi:10.1121/1.1908222)
23. Guckenheimer J, Holmes P. 1983 *Nonlinear oscillations, dynamical systems, and bifurcations of vector fields*. Applied Mathematical Sciences, vol. 42. New York, NY: Springer.
24. Glendinning P. 1994 *Stability, instability and chaos*. Cambridge, UK: Cambridge University Press.

Downloaded from https://royalsocietypublishing.org/ on 09 June 2021